Heliyon 5 (2019) e02758

Contents lists available at ScienceDirect

Heliyon

journal homepage: www.heliyon.com

Heliyon

Research article

Studies on nucleation and crystal growth kinetics of ferrous oxalate

Chuanbo Li, Yongzhi Ning, Taihong Yan, Weifang Zheng *

China Institute of Atomic Energy, P.O.Box 275-26, Beijing, 102413, China

ARTICLE INFO

Keywords:
Physical chemistry
Ferrous oxalate
Crystal growth rate
Dilution ratio
Nucleation rate

ABSTRACT

An improved apparatus is used for nucleation measurements according to Nielsen's method. A new method is proposed to calculate the dilution ratio *N* of the reaction solution during nucleation rate determination. With the rule, when the initial apparent supersaturation ratio $S'=f(N)$ in the dilution tank is controlled from 1.3 to 3.0, crystal nucleus dissolving and secondary nucleation can be avoided satisfactorily. Experiments are realized by varying the supersaturation ratio from 15.6 to 93.3 and temperature from 15 °C to 50 °C. Ferrous oxalate is precipitated by mixing equal volumes of ferrous sulfate and oxalic acid solution. The experimental results showed that the nucleation rate of ferrous oxalate in the supersaturation range above is characterized by the primary homogeneous mechanism and can be expressed by the equation $R_N = A_N exp(-E_a/RT) exp[-B/(\ln S)^2]$, where $A_N = 3.9\times10^{13}\ m^{-3}\ s^{-1}$, $E_a = 33.9$ kJ mol^{-1}, and $B = 13.7$. The crystal growth rate can be expressed by equation $G(t) = k_g exp(-E'_a/RT)\ (c\text{-}c_{eq})^g$, where $k_g = 3.6 \times 10^{13}$ m/s, $E'_a = 58.0$ kJ mol^{-1}, *and* $g = 2.4$.

1. Introduction

Ferrous oxalate is a simple metal organic framework co-ordinated polymer. Recently, ferrous oxalate has been extensively studied because of its applications in many fields [1, 2, 3, 4]. The synthesis plays an important role in uncovering their shape-dependent properties and fully achieving their potential practical applications. In spite of the fact that it is used in many fields, only few papers deal with the precipitation kinetics of ferrous oxalate. Abdel-Ghafar and Abdel-Aal [5] studied nucleation aspects and morphology of iron (II) oxalate dihydrate crystals in water and diluted phosphoric acid media. But the nucleation rate expression was calculated according to the equation reported in a handbook.

For the nucleation step, two reactive solutions are homogeneously and rapidly mixed in a short tube, where the high supersaturation generates primary nucleation. Then the solution is instantaneously diluted into a solution with stirring, where nuclei grow to the detectable size range. The dilution ratio must be suitable to avoid crystal nucleus dissolving, secondary nucleation and agglomeration in the dilution. The applications of this method are reported for determining precipitation kinetics by examples: hexahydrated tetravalent uranium oxalate [6], barium carbonate [7], struvite [8], gypsum [9]. However, the dilution ratio has not been mentioned in all the papers published and only the supersaturation ratios are shown. Even though, the supersaturation ratios in the dilution tank are different from each other in these papers, such as the supersaturation ratio 6 in [7], 1.83 ~ 3.44 in [8], 0.92 ~ 4.61 in [9] and no mentioned in [6]. For this reason, the objective of this article is to describe the method of achieving the dilution ratio, and to confirm the supersaturation ratio in the dilution tank.

1.1. Nucleation

According to the classical nucleation theory [10], the primary nucleation rate can be shown as follows:

$$R_N = B_{\text{hom}} = A\ \exp\left\{\frac{-B}{[\ln S]^2}\right\} \tag{1}$$

where R_N represents the number of nuclei formed per unit volume and time, A and B are the nucleation kinetic parameters and S is the supersaturation ratio defined as follows:

$$S = \frac{C_{Fe^{2+}}}{C_{Fe^{2+}equ}} \tag{2}$$

where $C_{(Fe2+)}$ is the concentration of ferrous in solution.

The nucleation rate is calculated from the total number of nuclei formed:

$$R_N = \frac{n}{V_{tube} \cdot t_{tube}} \tag{3}$$

* Corresponding author.
E-mail address: wfazh@ciae.ac.cn (W. Zheng).

https://doi.org/10.1016/j.heliyon.2019.e02758
Received 4 September 2018; Received in revised form 22 May 2019; Accepted 28 October 2019

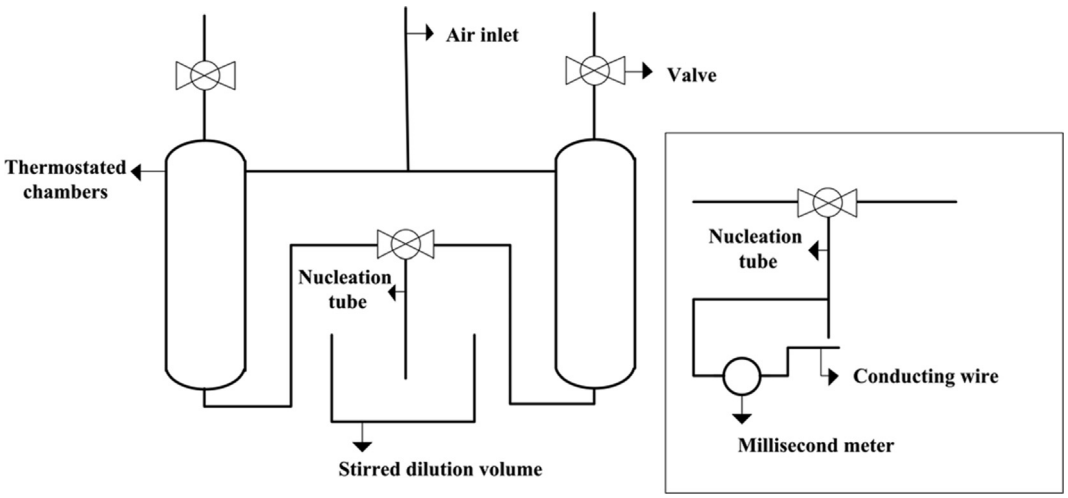

Fig. 1. The principle scheme of the apparatus for nucleation measurements.

where V_{tube} is the tube volume, t_{tube} is the nucleation process time and n is the total nuclei number. Eq. (1) is used to fit the experimental nucleation rate obtained from different supersaturation ratio values in order to get the kinetic parameters A and B.

1.2. Crystal growth

In a perfectly mixed batch reactor, where only the size-independent crystal growth occurs, the population density balance equation is [11]:

$$\frac{\partial n(L,t)}{\partial t} + G(t)\frac{\partial n(L,t)}{\partial L} = 0 \tag{4}$$

where L is the characteristic particle size, $n(L,t)$ is the population density and $G(t)$ is the crystal growth rate.

The following relation can be obtained [6]:

$$-\frac{d[Fe(II)]}{dt} = \frac{3n_S(t)\int_0^\infty \frac{g(L,t)}{L}dL}{V_L}G(t) \tag{5}$$

where $n_s(t)=V_sC_s(t)$, $n_s(t)$ is the solid particle mole number in the suspension, V_S and $C_s(t)$ are the suspension volume in the crystallizer and the solid concentration in the suspension, respectively, $g(L,t)$ is the initial mass size distribution of the seed charge in the suspension, V_L is the volume of solution.

Then the G(t) can be expressed by the following formula:

$$G(t) = -\frac{d[Fe(II)]}{dt}\frac{V_L}{3n_S(t)\int_0^\infty \frac{g(L,t)}{L}dL} \tag{6}$$

On the other hand, the crystal growth rate $G(t)$ is generally expressed as follows [12]:

$$G(t) = K_g\Delta C^r = K_g\,(C_{(Fe2+)} - C_{(Fe2+)equ})^g \tag{7}$$

where k_g is the kinetic constant, $C^{2+}_{(Fe)}$ and $C^{2+}_{(Fe)equ}$ are the initial and equilibrium concentrations of ferrous in solution.

1.3. Dilution ratio in nucleation

During the nucleation, the dilution ratio in the tank must be suitable to avoid crystal nucleus dissolving, secondary nucleation and agglomeration in the dilution tank occuring. The dilution ratio depends on the concentrations of ferrous and oxalate acid. A new method is proposed to calculate the dilution ratio. If the two reaction solutions were diluted by the solution in the tank directly without passing through the nucleation tube, then the initial apparent supersaturation ratio S' in the dilution tank was:

$$S' = \sqrt[m+n]{\frac{\left[\frac{c_{Fe^{2+}}}{2N}\right]^m \cdot \left[\frac{c_{C2O4^{2-}}}{2N}\right]^n}{c^m_{Fe^{2+}equ}\cdot c^n_{C2O4^{2-}equ}}} \tag{8}$$

where $C^{2+}_{(Fe)}$ and $C^{2-}_{(C2O4)}$ are the concentrations of ferrous and oxalate in solution, respectively, m,n are stoichiometry values, $m=n=1$, N is dilution ratio. Then N can be expressed by:

$$N = \frac{\sqrt[m+n]{\frac{c^m_{Fe^{2+}}\cdot c^n_{C2O4^{2-}}}{c^m_{Fe^{2+}}equ\cdot c^n_{C2O4^{2-}}equ}}}{2S'} \tag{9}$$

2. Experimental

2.1. Materials

Ferrous oxalate precipitation is performed by the chemical reaction in aqueous solution between ferrous sulfate and oxalic acid:

$$FeSO_4 + H_2C_2O_4 + 2H_2O \rightarrow Fe\ C_2O_4{\cdot}2H_2O + H_2SO_4 \tag{10}$$

0.10 mol/L $N_2H_4{\cdot}HNO_3$ is added to the ferrous sulfate solution to stabilize the ferrous ion for 60 days. The ferrous sulfate solution contains more than 99.9% ferrous.

The micro-concentration of ferrous is determined by the colour reaction between Fe^{2+} and 1,10-Phenanthroline. A preliminary study is carried out for the determination of ferrous oxalate solubilities under different conditions.

Table 1
The dilution ratio in ferrous oxalate nucleation rate deteimination.

T	$c(Fe^{2+})_0$/(mol/L)	$c(H_2C_2O_4)_0$/(mol/L)	S	S′	N	Nucleation time/(ms)
25°C	0.15	0.35	46.7	0.8	11.0	17.7
	0.15	0.35	46.7	1.0	9.0	17.7
	0.15	0.35	46.7	1.3	7.0	17.7
	0.15	0.35	46.7	1.5	6.0	17.7
	0.15	0.35	46.7	1.8	5.0	17.7
	0.15	0.35	46.7	2.3	4.0	17.7
	0.15	0.35	46.7	3.0	3.0	17.7
	0.15	0.35	46.7	3.6	2.5	17.7
	0.15	0.35	46.7	4.5	2.0	17.7
	0.15	0.35	46.7	6.0	1.5	17.7

Table 2
The ferrous oxalate nucleation rate determination conditions.

T	$c(Fe^{2+})_0$/(mol/L)	$c(H_2C_2O_4)_0$/(mol/L)	S	S′	N	Nucleation time/(ms)
25 °C	0.30	0.50	93.3	1.5	10.2	17.7
	0.20	0.40	62.2	1.5	7.5	17.7
	0.15	0.35	46.7	1.5	6.1	17.7
	0.090	0.29	28.0	1.4	4.5	17.7
	0.070	0.27	21.8	1.4	3.9	17.7
	0.050	0.25	15.6	1.3	3.3	17.7
35 °C	0.070	0.27	17.8	1.6	3.9	17.7
45 °C	0.070	0.27	17.8	1.6	3.9	17.7
50 °C	0.070	0.27	16.3	1.5	3.9	17.7

Table 3
The ferrous oxalate crystal growth rate deteimination conditions.

T	$c(Fe^{2+})_0$/(mol/L)	$c(H_2C_2O_4)_0$/(mol/L)	S	S′	N	Nucleation time/(ms)
25 °C	0.070	0.27	21.8	1.4	3.9	17.7
	0.070	0.27	21.8	1.8	3.0	17.7
	0.070	0.27	21.8	2.1	2.6	17.7
	0.070	0.27	21.8	2.4	2.3	17.7
	0.070	0.27	21.8	2.8	1.9	17.7
15 °C	0.070	0.27	28.0	1.7	3.1	17.7
35 °C	0.070	0.27	17.8	1.6	3.1	17.7
45 °C	0.070	0.27	17.8	1.5	3.1	17.7

2.2. Experimental apparatus

Söhnel and Mullin [13] has proposed a "stopped-flow'' method to study the primary nucleation. In this paper, an improved apparatus is used to for the determination of the nucleation rate. The basic operating principle is schematically shown in Fig. 1a. Reactants are placed in two thermostated chambers. The two reactant solutions are rapidly and simultaneously pushed into the nucleation tube via 0.52MPa pressure air. The air is filtrated by pure water to remove the dust particles. In the nucleation tube, reactants are mixed and the high supersaturation initiates nucleation. The nucleation tube is a T-tube mixing device, the diameters of two inlet tubes and the outlet tube are all 2.0mm. At the exit of the tube, the nucleation is stopped by the stirred dilute solution in the square vessel.

The nucleation time is an important parameter influencing the determination of nucleation rate. A millisecond counter device is used to measure the injection time, as shown in Fig. 1b. Switch of the millisecond counter device is controlled by the solution coming down from the nucleation tube.

2.3. Experimental procedure

(1) Dilution ratio in nucleation

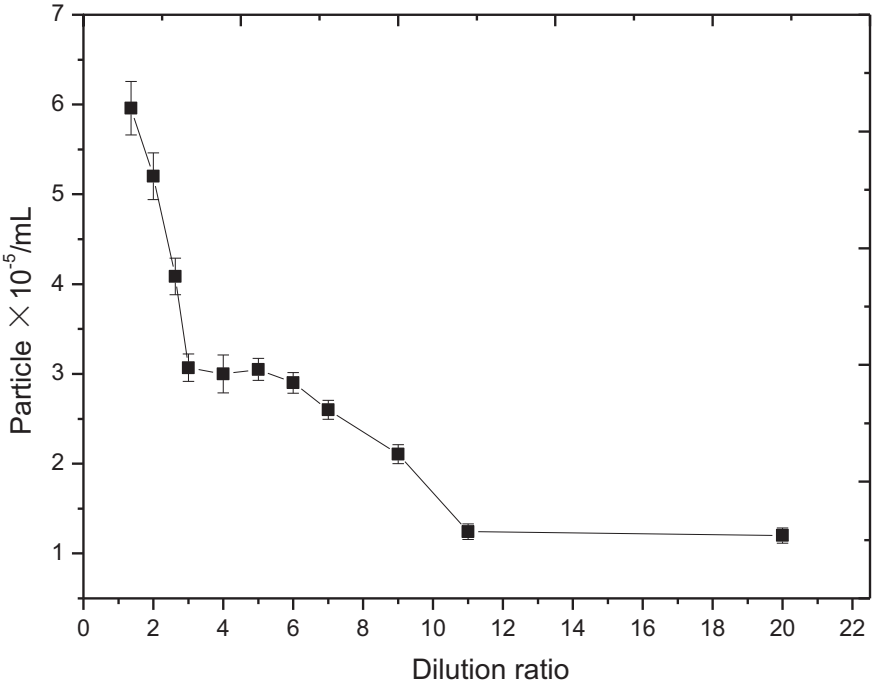

Fig. 2. The effect of *N* on nucleation rate in nucleation.

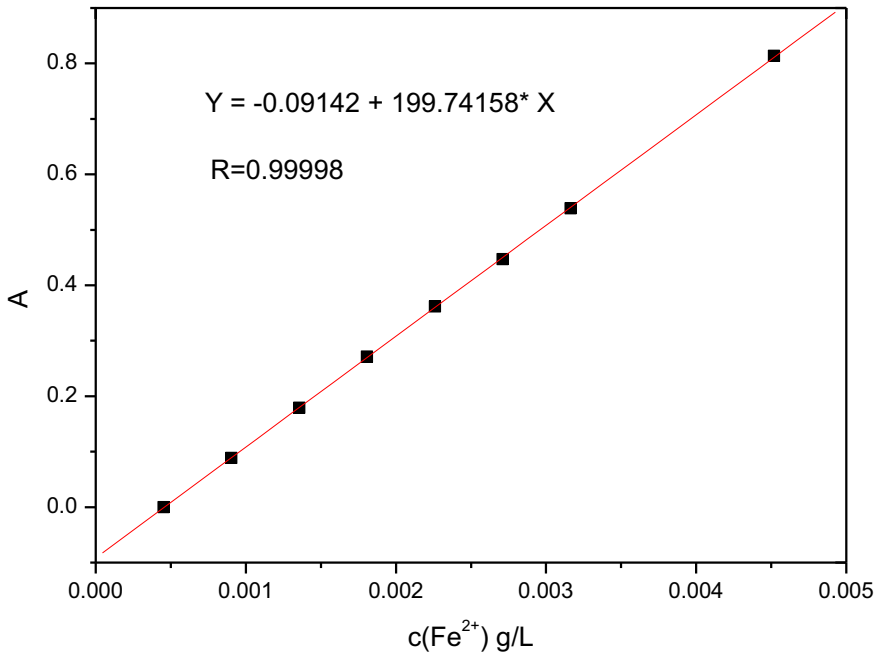

Fig. 3. The effect of c(Fe^{2+}) with 1,10-Phenanthroline on A.

Table 4
The ferrous oxalate solubilities under different conditions.

	Fe^{2+} (g/L)				
Solution system	15 °C	25 °C	35 °C	45 °C	50 °C
0.10 mol/L $H_2C_2O_4$ + 0.10 mol/L N_2H_4•HNO_3 + 0.15 mol/L H_2SO_4	0.069	0.090	0.11	0.11	0.12

The nucleation of ferrous oxalate is got experimentally by rapid simultaneous mixing 15.0ml ferrous sulfate (0.15 mol/L $FeSO_4$+0.10 mol/L N_2H_4•HNO_3+0.075 mol/L H_2SO_4) and 15.0ml oxalic acid (0.35 mol/L $H_2C_2O_4$+0.10 mol/L N_2H_4•HNO_3+0.075 mol/L H_2SO_4) in the nucleation tube via 0.52MPa pressure. The two solutions are initially heated to the preconcerted temperature. Experiments are realized by varying *S'* from 0.3 to 6.0, with *N* from 30 to 1.5, at the temperature of 25 °C, as shown in Table 1.

Then the mixture is rapidly diluted by the stirred dilute solution (0.10 mol/L $H_2C_2O_4$+0.10 mol/L N_2H_4•HNO_3+0.15 mol/L H_2SO_4) in a 250ml vessel to stop further nucleation. The initial rotating speed is 3000 rpm and then turns to 300 rpm in 10 s. The initial *S* is 46.7. The nuclei generated grow in the dilution tank using the remaining material. The particle growth time is 5 min, growing to the suitably detected size. After the crystal growth, an ultrasonic probe is used to break the partially agglomerated ferrous oxalate particles. Then the number of crystals

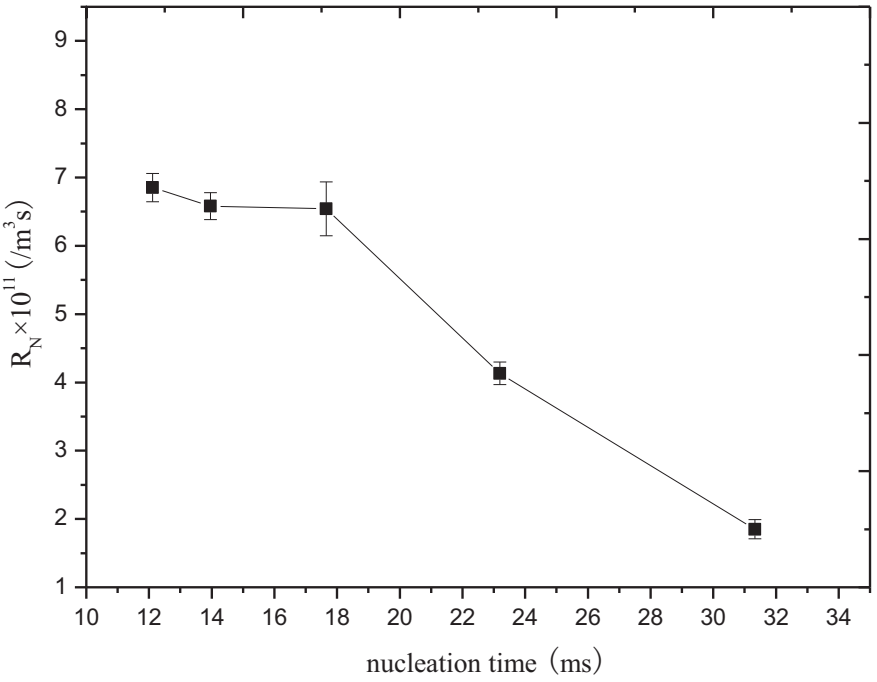

Fig. 4. Effect of nucleation time on nucleation rate.

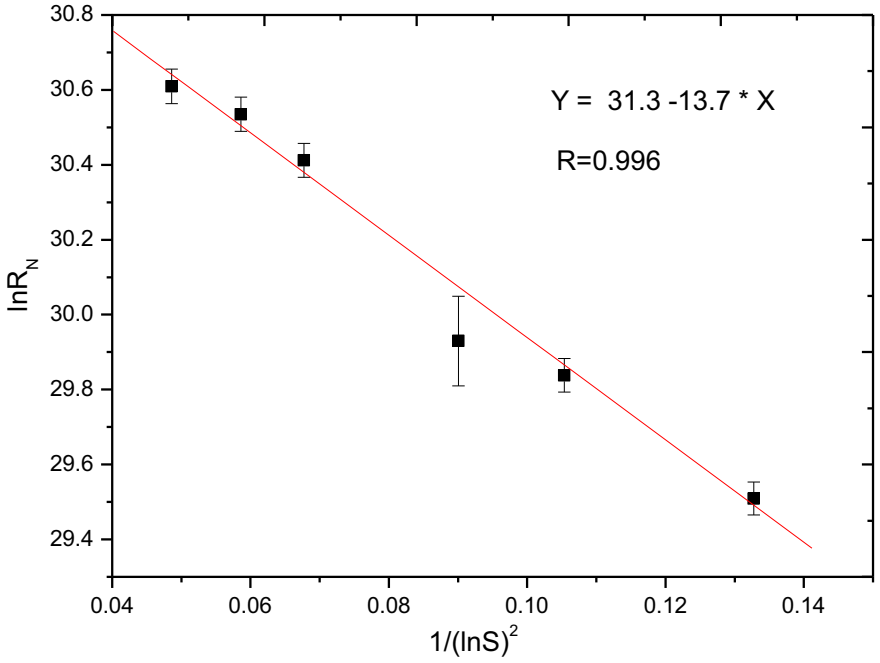

Fig. 5. Primary nucleation kinetics as a function of supersaturation ratio at 25 °C.

during the nucleation is calculated by the particle counter apparatus. The mixing time of 50mL solution is 2.60s measured by the millisecond counter device. This time corresponds to a flow rate of 19.2 ml s^{-1} and the nucleation time of 17.7 ms.

(2) Determination of nucleation rate

As above, the nucleation of ferrous oxalate is got experimentally by rapid simultaneous mixing 15.0–20.0ml ferrous sulfate (0.05–0.30 mol/L $FeSO_4$+0.10 mol/L N_2H_4•HNO_3+0.125–0 mol/L H_2SO_4) and 15.0–20.0ml oxalic acid (0.25–0.50 mol/L $H_2C_2O_4$+0.10 mol/L N_2H_4•HNO_3+0.125–0 mol/L H_2SO_4) in the nucleation tube via 0.52MPa pressure. Experiments are realized by varying the supersaturation ratio from 15.6 to 93.3 and at the temperature of 25 °C–50 °C, as shown in Table 2. The *S'* is controlled between 1.3 to 1.6, with *N* from 3.3 to 10.2. The initial *S* is from 15.6 to 93.3.

(3) Determination of crystal growth rate

For continuous precipitation operations are usually applied in industry to get a stable product, the ferrous oxalate crystal nucleus created in the tube during nucleation are used as the seed charge to simulate the conditions in the industry crystallizers. The ferrous oxalate crystal nucleus are got experimentally by rapid simultaneous mixing 15.0ml ferrous sulfate (0.070 mol/L $FeSO_4$+ 0.10 mol/L N_2H_4•HNO_3+0.115 mol/L H_2SO_4) and 15.0ml oxalic acid (0.27 mol/L $H_2C_2O_4$+ 0.10 mol/L N_2H_4•HNO_3+0.115 mol/L H_2SO_4) in the nucleation tube via 0.52MPa pressure. Each solution with ferrous oxalate crystal nucleus obtained

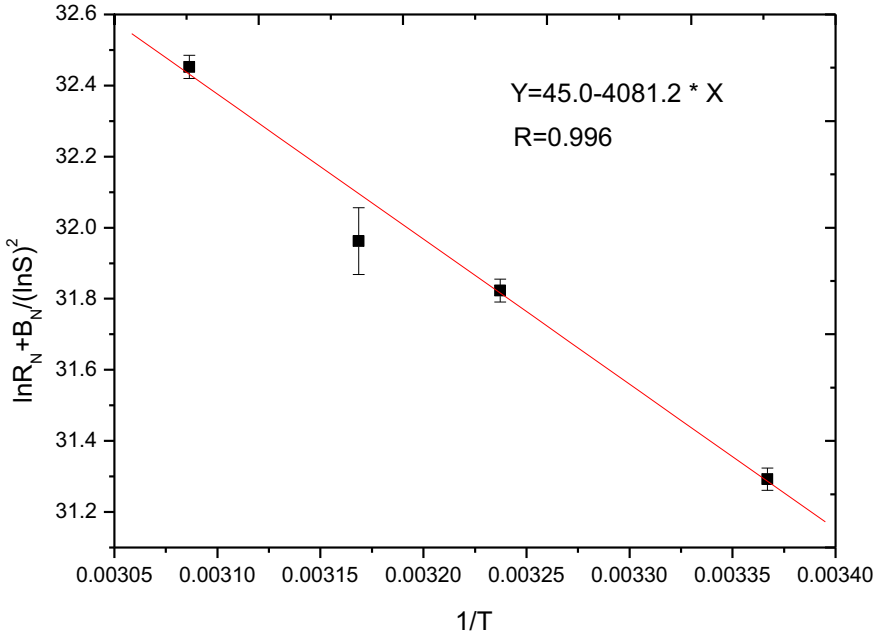

Fig. 6. Temperature influence on primary nucleation.

above is put into a 250ml vessel, stirred and initially filled with the dilute solution (0.10 mol/L $H_2C_2O_4$+0.10 mol/L N_2H_4•HNO_3+0.15 mol/L H_2SO_4). The crystal nucleus size distribution is measured by a laser particle size analyzer in 5.0 min. An injector with a 0.22 μm filter membrane allows to sample the aqueous phase every 30 min. The particle growth time is about 5 h. The colour reaction between ferrous and 1,10-Phenanthroline is used to determine the micro-concentration of the ferrous in the aqueous phase.

Experiments are realized by varying the temperature from 15 °C to 45 °C. The *S'* is controlled between 1.4 to 2.8, with *N* from 2.1 to 3.9 and the initial *S* in the dilution tank from 17.8 to 28.0, as shown in Table 3.

3. Results and discussion

3.1. Dilution ratio in nucleation

The effect of *N* on nucleation rate in nucleation is shown in Fig. 2. It shows that when *N* is from 7.0 to 3.0, with *S'* from 1.3 to 3.0, the nucleation rate increases slowly and *N* is feasible to avoid crystal nucleus dissolving, secondary nucleation in the dilution.

3.2. Nucleation rate determination

The solubility of ferrous oxalate is an important value for nucleation rate determination. The micro-concentration of ferrous is determined by the colour reaction with 1,10-Phenanthroline and the calibration curve is in Fig. 3. The ferrous oxalate solubilities under different conditions determined by us are shown in Table 4.

The effect of the nucleation tube length on nucleation rate is shown in Fig. 4. It shows that the agglomeration is obvious when the nucleation time is more than 23 ms. The nucleation time is no more than17.7 ms in the experiments of nucleation rate determination.

Eq. (1) is used to fit the experimental data obtained from different initial ferrous concentrations. Fig. 5 shows the nucleation rate plotted against $1/(lnS)^2$, which is obtained at 25°Cfor supersaturation ratio values varying from 15.6 to 93.3, the correlation coefficient is 0.988. The mathematical treatment of the experimental data obtained at 25 °C gives the following homogeneous nucleation rate:

$$R_N = B_{\text{hom}} = 3.9 \times 10^{13} \text{m}^{-3} s^{-1} \exp\left\{\frac{-13.7}{[\ln S]^2}\right\} \tag{11}$$

Nucleation is sensitive to temperature. The kinetic parameter *B* [10] is practically temperature independent for temperature variations between 25 °C and 50 °C [14]. While the kinetic parameter A_N depends on the temperature according to an Arrhenius expression:

$$A = A_0 \exp\left\{\frac{-E_a}{RT}\right\} \tag{12}$$

Therefore, the variation of the nucleation kinetics with temperature is mainly due to the pre-exponential factor variation. Fig. 6 shows the $[\ln R_N + B/(\ln S)]$ plotted against $1/T$, which is obtained from temperature variations between 25 and 50 °C, the correlation coefficient is 0.988. So homogeneous primary nucleation rate can be expressed by the following formula:

$$R_N = B_{\text{hom}} = 3.5 \times 10^{19} \text{m}^{-3} s^{-1} \exp\left\{\frac{-33.9 KJ/mol}{RT}\right\} \exp\left\{\frac{-13.7}{[\ln S]^2}\right\} \tag{13}$$

3.3. Crystal growth rate determination

Experiments are carried out as described in section 3.3(2). At 25 °C, when *N* in the dilution tank is controlled from 2.1 to 3.9, the decrease of ferrous concentrations in different dilute solutions are shown in Fig. 7. Based on the influence of *t* on the ferrous concentrations *c* in Fig. 7, when t ~ 0 the value of *dc/dt* can be gained by differentiating for each curve.

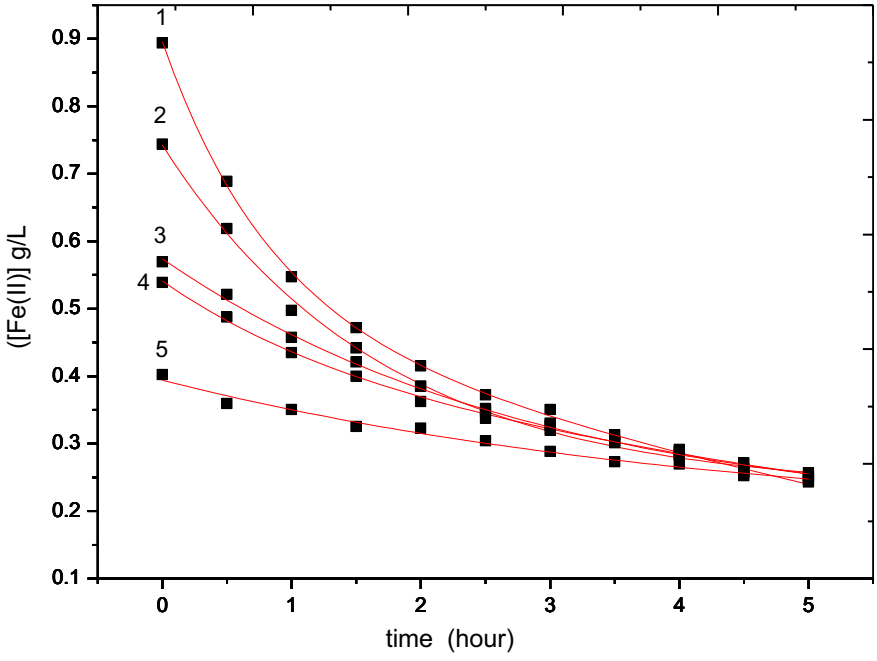

Fig. 7. Influence of time on ferrous concentrations at 25 °C. The dilution ratio: 1, 2.1; 2, 2.3; 3, 2.6; 4, 3.1; 5, 3.9.

The experimental data deals with Eqs. (6) and (7) shows that the growth rate is 2.4 order with respect to (C-C_{equ}), as shown in Fig. 8. Then at 25 °C the following growth kinetic law is derived.

$$G = K_g\,(C\text{-}C_{equ})^g = 33.1(\text{mol/L})^{-2.4}(\text{m/s})\,(C\text{-}\,C_{equ})^{2.4} \tag{14}$$

Temperature studies show that the crystal growth kinetic constant variation with temperature can be well expressed using an Arrhenius type equation. The experimental data treatment according to Eqs. (6), (7), and (10) shows the *[lnG-2.4ln(c-c_{eq})]* plot against *1/T* for temperatures varying from 15 °C to 45 °C, as Fig. 10. From these data, the following expression is obtained:

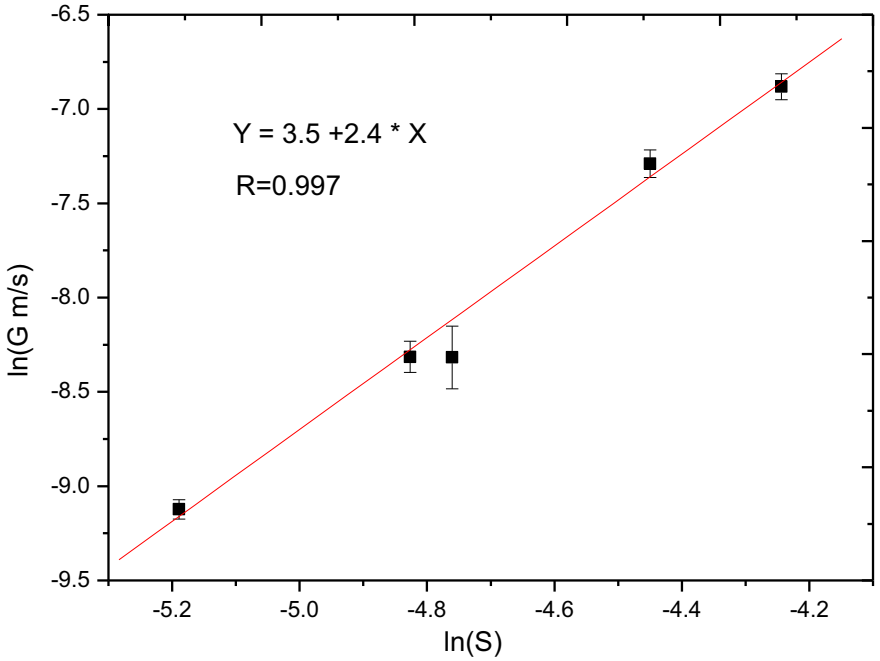

Fig. 8. Influence of ln(C- C_{equ}) on ln$G$ at 25 °C.

Experiments are carried out as described in section 3.3(2). From 15 °C to 45 °C, when N in the dilution tank is controlled to 3.1, S' 1.4 to 1.7, the decrease of ferrous concentrations in different solutions are shown in Fig. 9. Based on the influence of t on the ferrous concentrations c in Fig. 9, when $t \sim 0$ the value of dc/dt can be gained by differentiating of each curve.

$$G = \mathrm{k_g}\exp\left\{\frac{-E_a'}{RT}\right\}(c-c_{eq})^g = 3.6\times10^{13}\,(\text{mol/}L)^{-2.4}(m/s)\exp\left\{\frac{-58.0KJ/mol}{RT}\right\}(c-c_{eq})^{2.4} \tag{15}$$

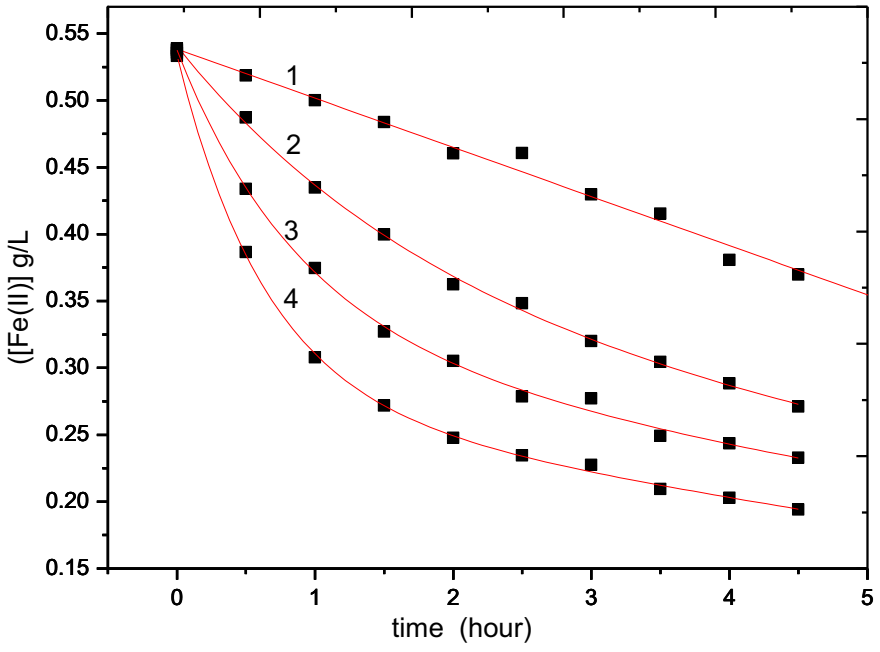

Fig. 9. Influence of time on ferrous concentrations from 15 °C to 45 °C.

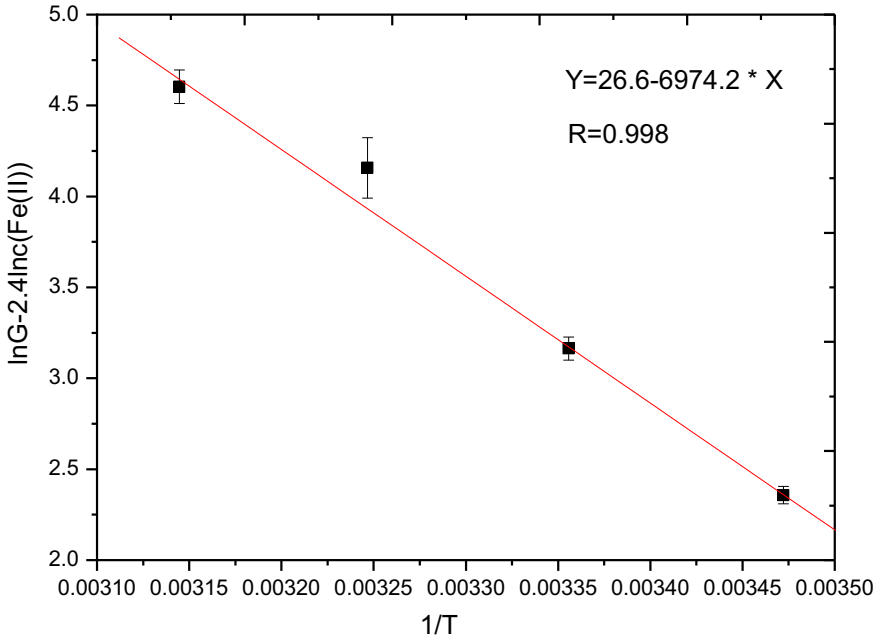

Fig. 10. Influence of [ln$G$-2.4ln(c-c_{eq})] plot on 1/T from 15 °C to 45 °C.

Bhat et al. [16] carried out a correlation between applied elastic stress and reduction in growth velocity of large potash alum crystals. The more the crystal was stressed the less it grew. A growth retardation effect due to the presence of lattice strain and deformation was also discovered for the crystallizing systems Rochelle salt [17] and proteins [18]. Meadhra et al. [19] investigated the kinetic behaviour of fines of ammonium sulphate produced in a crystalliser. The results supported the hypothesis that the increased level of internal strain in fragments produced by attrition reduced the growth rates of the crystals.

To simulate the continuous precipitation operations in the industry, the ferrous oxalate crystal nucleus created in the tube during nucleation are used as the seed charge. The mass percentage of the crystal nucleus is 14%–21% of the product particles in the dilution tank. The internal strain and deformation in particles produced by attrition from stirring reduced the growth rates of the crystals and make the activation energy crystal growth of ferrous oxalate is higher than that of nucleation.

4. Conclusion

An improved apparatus is used for nucleation measurements according to Nielsen's method. And a new method is proposed to calculate the dilution ratio of the reaction solutions during nucleation rate determination. The method is successfully used here for the determination of nucleation rate expression of ferrous oxalate. With the rule, when the initial apparent supersaturation ratio S' in the dilution tank is controlled from 1.3 to 3.0, crystal nucleus dissolving and secondary nucleation can be avoided satisfactorily. To simulate the continuous precipitation operations in the industry crystallizers, the ferrous oxalate crystal nucleus created in the tube during nucleation are used as the seed charge and the growth kinetics of ferrous oxalate is also obtained.

Declarations

Author contribution statement

Chuanbo Li: Conceived and designed the experiments; Performed the experiments; Analyzed and interpreted the data; Wrote the paper.

Yongzhi Ning: Performed the experiments; Contributed reagents, materials, analysis tools or data Taihong Yan: Analyzed and interpreted the data.

Weifang Zheng: Conceived and designed the experiments; Analyzed and interpreted the data.

Competing interest statement

The authors declare no conflict of interest.

Funding statement

This research did not receive any specific grant from funding agencies in the public, commercial, or not-for-profit sectors.

Additional information

No additional information is available for this paper.

References

[1] C.M. Doherty, R.A. Caruso, B.M. Smarsly, et al., Colloidal crystal templating to produce hierarchically porous $LiFePO_4$ electrode materials for high power lithium ion batteries, Chem. Mater. 21 (3) (2009) 2895–2903.
[2] J.P. Dhal, B.G. Mishra, G. Hota, Ferrous oxalate, maghemite and hematite nanorods as efficient adsorbents for decontamination of Congo red dye from aqueous system, Int. J. Env. Sci. Technol. 12 (6) (2015) 1845–1856.
[3] A. Angermann, J. Toepfer, Nanocrystalline Mn–Zn ferrites from mixed oxalates: synthesis, stability and magnetic properties, J. Mater. Sci. 508 (2) (2010) 433–439.
[4] Michel Vedrenne, Ruben Vasquez-Medrano, A ferrous oxalate mediated photo-Fenton system: toward an increased biodegradability of indigo dyed wastewaters, J. Hazard Mater. 243 (2012) 292–301.
[5] H.M. Abdel-Ghafar, E.A. Abdel-Aal, Studying nucleation aspects and morphology of iron (II) oxalate dihydrate crystals in water and diluted phosphoric acid media, Egypt. J. Pet. 27 (4) (2018) 1235–1240.
[6] Murielle Bertrand-Andrieu, Edouard Plasari1, Pascal Baron, Determination of nucleation and crystal growth kinetics in hostile environment – application to the tetravalent uranium oxalate $U(C_2O_4)_2$ $6H_2O$, Can. J. Chem. Eng. 82 (5) (2004) 930–938.
[7] Fabien Salvatori, Hervé Muhr, Edouard Plasari, Determination of nucleation and crystal growth kinetics of barium carbonate, Powder Technol. 128 (2002) 114–123.
[8] Mary Hanhoun, Ludovic Montastruc, Catherine Azzaro-Pantel, Simultaneous determination of nucleation and crystal growth kinetics of struvite using a thermodynamic modeling approach, Chem. Eng. J. 215–216 (2013) 903–912.
[9] E. Barbier, M. Coste, A. Genin, Simultaneous determination of nucleation and crystal growth kinetics of gypsum, Chem. Eng. Sci. 64 (2009) 363–369.
[10] M. Volmer, A. Weber, Keimbildung in ûbersâttingen gebilden, Zeitschrift für Phyikalische Chemie. 119 (1926) 277–301 (Martell and Motekaitis, 1992, J. Rydberg et al., 1992.).

[11] A.D. Randolph, M.A. Larson, Theory of Particulate Processes, second ed., Academic Press, New York, NY, 1988.
[12] A. Nielsen, Nucleation and growth of crystals at high supersaturations, Krist. Tech. 4 (1969) 17–32.
[13] O. Söhnel, J.W. Mullin, A method for the determination of precipitation induction periods, J. Cryst. Growth 44 (1978) 377–382.
[14] A. Mersmann, Calculation of interfacial tensions, J. Cryst. Growth 102 (1990) 841–847.
[16] H.L. Bhat, J.N. Sherwood, T. Shripathi, The influence of stress, strain and fracture of crystals on the crystal growth process, Chem. Eng. Sci. 42 (1987) 609.
[17] M.M. Mitrovic, Growth rate dispersion of small Rochelle salt crystals, J. Cryst. Growth 85 (1987) 411.
[18] S.J. Andrews, J.E. Hails, M.M. Harding, The mosaic spread of very small crystals deduced from laue diffraction patterns, Acta Crystallogr. A 43 (1987) 70.
[19] R.S. Ó Meadhra, H.J.M. Kramer, G.M. van Rosmalen, Size dependent growth behaviour related to the mosaic spread in ammonium sulphate crystals, J. Cryst. Growth 152 (1995) 314.